electronics

MDPI

Article

CSI-Impaired Beamforming Optimization for Dense MIMO Communication Networks

Bencheng Yu [1,2,*], Zihui Ren [1] and Shoufeng Tang [1]

[1] School of Information and Control Engineering, China University of Mining and Technology, Xuzhou 221116, China
[2] Xuzhou College of Industrial Technology, Xuzhou 221140, China
* Correspondence: yubc@mail.xzcit.cn

Abstract: This paper studied the robust beamforming for dense transmission systems with imperfect channel state information (CSI). The objective was to maximize the minimum signal to interference plus noise ratio (SINR) in the constraint of the per base station (BS) power. By performing the uplink–downlink duality theory, the referred non-convex optimization problem can be changed into the equivalent uplink decoupling optimization problem. Then, we proposed the instantaneous updating uplink–downlink power algorithm, which relies on instantaneous CSI for the finite system. For the massive MIMO system, to obtain the solution to the problem required for power to instantaneously update, we proposed the updating uplink–downlink power algorithm, which only requires statistical CSI, by applying the random matrix theory. The simulation results show the feasibility and effectiveness of our proposed algorithms.

Keywords: power control; coordinated multi-cell beamforming; uplink–downlink duality; random matrix theory

Citation: Yu, B.; Ren, Z.; Tang, S. CSI-Impaired Beamforming Optimization for Dense MIMO Communication Networks. *Electronics* **2022**, *11*, 3225. https://doi.org/10.3390/electronics11193225

Academic Editor: Ahmed Al Durra

Received: 13 September 2022
Accepted: 1 October 2022
Published: 8 October 2022

1. Introduction

In the future, 6G mobile communication data traffic will dramatically increase [1–3]. Compared with increasing spectrum bandwidth and improving physical layer technology, Ultra-Dense Networks (UDN) improve network coverage through hhigh-density frequency space reuse, which is a more effective way to improve spectrum utilization and wireless network capacity [4–6]. However, network densification has led to a continuous increase in the number of base stations that cause co-channel interference to target users [7], and inter-cell interference has become the main factor restricting the growth in network capacity. Therefore, without considering the limited network resources (backhaul capacity [8], data transmission delay [9], etc.), there is a basic density limit for ultra-dense networking. Adding more base stations per unit area (or per unit volume) will not help improve network performance.

Recently, multiple-input–multiple-output (MIMO) has become a promising approach to enhance the throughput of wireless communication systems. However, inter-cell interference also becomes a serious problem, which heavily impacts system performance. To reduce inter-cell interference, coordinated multiple point (CoMP) technology has been extensively studied [10,11]. By sharing channel information and user data information, multiple base stations provide services for the same user at the same time, and the interference between adjacent cells changes from passive suppression to active utilization, which can effectively reduce the interference between cells [12], and has wide application prospects in ultra-dense networking [13]. The cooperation mode without channel state information-sharing is far less effective than the joint transmission of shared channel state information [14]. Reference [15] divides cells with strong interference into a cluster to share spectrum resources, cooperate to serve users, and implement spectrum reuse between clusters to reduce interference. References [16,17] use multi-point cooperation technology

to improve the uplink condition to reduce the base station density in the network models of the regular deployment and random deployment of base stations, respectively, and obtain an accurate closed-form solution for the total coverage rate of each base station in the cooperation area. At the same time, based on the bounded dual-slope path loss model, reference [18] analyzes the improvement in user coverage obtained by multi-point cooperative joint transmission after the user only selects the two nearest base stations as cooperative base stations after the omni-directional single-antenna base station is randomly deployed. Reference [19] divides a regular hexagonal grid on the plane of randomly deployed base stations. The base stations in a grid form a cooperative cluster, and stochastic geometry and large deviation theory are used to analyze the communication outage rate of mobile users. Reference [20] considers that when the base station density is greater than the user density, nearby idle base stations are used for multi-point cooperative transmission, and then studies the impact of different amounts of cooperation on the network's energy efficiency. However, research on the impact of base station density on network performance in ultra-dense networking under the condition of multi-point cooperative joint transmission is still lacking.

For the Time-Division Duplexing (TDD) downlink multi-cell system, a distributed hierarchical algorithm was proposed in [21] to optimize the beamforming vector and power distribution, and the algorithm only requires a limited exchange message. To solve the joint beamforming problem, a two-step centralized algorithm is introduced in [22] to improve the rate performance. In [23], the goal of the design is to obtain the max–min SINR. A hierarchical virtual uplink iterative algorithm is also proposed to obtain the solution of the optimization problem, and the proposed algorithm has a better performance in terms of energy efficiency and the rate of the worst user; thus, the coordinated beamforming was solved for the multi-cell multi-input–single-output (MU-MISO) system. To leverage the uplink–downlink duality, the SINR-balancing problem was first addressed in [24] using the extended coupling matrix.

Most works in the literature mentioned above only focus on the ideal independent channel and assume that the BS knows the CSI. Due to the time-varying channel, channel bandwidth and the different means of obtaining the CSI for the actual system, the assumption of the above works does not hold. Furthermore, little research to date has addressed the combination of beamforming designing and power control for fairness among users with an imperfect CSI, subject to some constraints in coordinated multi-cell systems.

Inspired by the above results, in this paper, we focus on fairness among users, formulated by maximizing the minimum SINR within the constraints of the per-BS power with an imperfect CSI. Then, the non-convex downlink optimization problem is transformed into an equivalent uplink optimization form using the uplink–downlink theory. To solve the instantaneous update power with instantaneous power for the finite system, the algorithm that only requires statistical CSI to update power, which can obtain the beamformer without iterations, was proposed for the massive MIMO system. Numerical results test the effectiveness of our developed algorithms and show the advantages of our proposed algorithms compared to maximal-ratio transmit within the per-BS power constraints.

2. System Model

As shown in Figure 1, we consider a K-cell MU-MISO downlink transmission network, where the j-th BS has M_j transmit antennas and I users are equipped with a single-antenna in cell j, $j = 1, \ldots, K$. User-(j,k) represents the k-th receiver of the cell j. Then, the received signal $y_{j,k}$ of user-(j,k) is

$$y_{j,k} = \sum_{m=1}^{K} \sum_{n=1}^{I} \sqrt{p_{m,n}} \mathbf{h}_{m,j,k}^{H} \hat{\mathbf{w}}_{m,n} x_{m,n} + n_{j,k} \tag{1}$$

where $p_{j,k}$ and $x_{j,k}$ denote the transmit power and the information signal, respectively, from the BS to user-(j,k), $\mathbf{h}_{m,j,k}$ is the communication channel between the m-th BS and

user-(j,k), $\hat{\mathbf{w}}_{j,k}$ denotes the transmit beamforming for user-(j,k) ($||\hat{\mathbf{w}}_{j,k}|| = 1$), and $n_{j,k}$ is the additional noise, considering the Gaussian distribution.

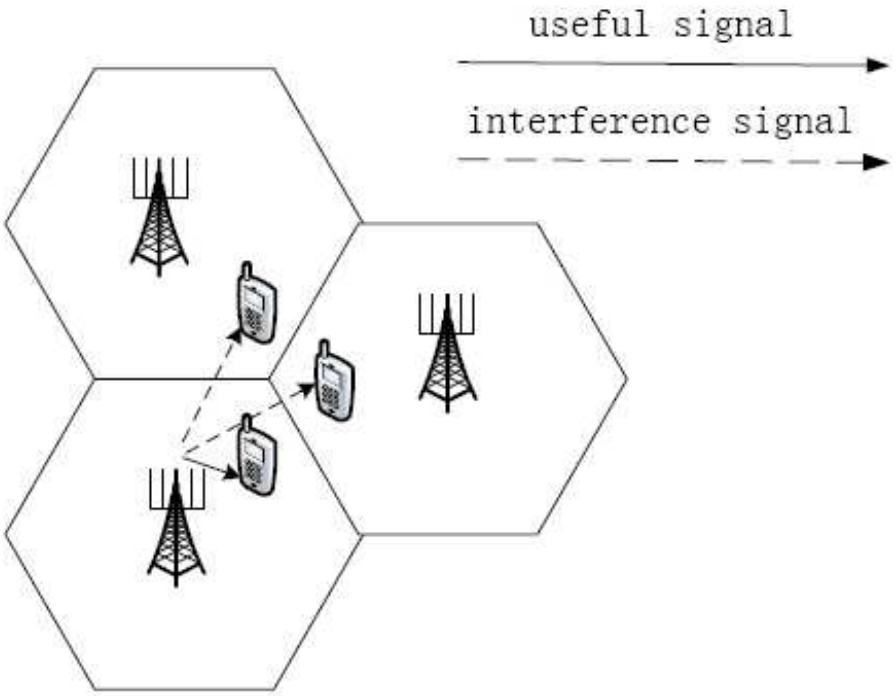

Figure 1. System model.

Following the results of [12], $\mathbf{h}_{m,j,k}$ is modeled as

$$\mathbf{h}_{m,j,k} = \mathbf{\Phi}_{m,j,k}^{\frac{1}{2}} \mathbf{z}_{m,j,k} \tag{2}$$

where $\mathbf{h}_{m,j,k} \sim \mathcal{CN}\left(0, \frac{d_{m,j,k}\mathbf{R}_{m,j,k}}{M_m}\right)$, $\mathbf{z}_{m,j,k} \sim \mathcal{CN}(0, \mathbf{I}_{M_m})$, $d_{m,j,k}$ is the large-scale factor, and $\mathbf{R}_{m,j,k} \in \mathbb{C}^{M_m \times M_m}$ meets the conditions, as follows:

$$\lim sup \left\| \mathbf{R}_{m,j,k} \right\| < +\infty, \forall m, j, k$$

$$\lim inf \frac{1}{M_m} tr\left(\mathbf{R}_{m,j,k}\right) > 0, \forall m, j, k$$

Here, we assume that only an imperfect channel was available at the m-th transmitter. Therefore, this can be modeled by [25] as

$$\begin{aligned} \hat{\mathbf{h}}_{m,j,k} &= \mathbf{\Phi}_{m,j,k}^{\frac{1}{2}} \left(\sqrt{1-\tau^2} \mathbf{z}_{m,j,k} + \tau \boldsymbol{\chi}_{m,j,k} \right) \\ &= \sqrt{1-\tau^2} \mathbf{h}_{m,j,k} + \tau \mathbf{n}_{m,j,k} \end{aligned} \tag{3}$$

where $\mathbf{h}_{m,j,k}$ represents the actual channel, $\boldsymbol{\chi}_{m,j,k} \sim \mathcal{CN}(\mathbf{0}; \mathbf{I}_{M_m})$, $\mathbf{n}_{m,j,k} = \mathbf{\Phi}_{m,j,k}^{\frac{1}{2}} \boldsymbol{\chi}_{m,j,k} \sim \mathcal{CN}\left(\mathbf{0}, \frac{d_{m,j,k}}{M_m} \mathbf{R}_{m,j,k}\right)$ models the channel error. The parameter $\tau \in [0,1]$ refers to the quality of the instantaneous CSI.

The considered K-cell MU-MISO broadcasting channel (1) can be essentially referred to as an interference systems with $\bar{I} = KI$ receivers, by which user-$\left(\lceil \frac{m}{I} \rceil, m - I\lfloor \frac{m}{I} \rfloor\right)$ can simply be denoted as user-m, with $\lceil \cdot \rceil$ and $\lfloor \cdot \rfloor$ denoting the ceiling and floor function, respectively. Thus, several new parameters are defined as: let $\hat{\mathbf{h}}_{n,m} = \hat{\mathbf{h}}_{\lceil \frac{n}{I} \rceil, \lceil \frac{m}{I} \rceil, m - I\lfloor \frac{m}{I} \rfloor}$ denote the channel with channel estimation error from the BS-n to the user-m; let $\mathbf{h}_{n,m} = \mathbf{h}_{\lceil \frac{n}{I} \rceil, \lceil \frac{m}{I} \rceil, m - I\lfloor \frac{m}{I} \rfloor}$ denote the channel parameter from the BS-n to the user-m; let $p_m =$

$p_{\lceil \frac{m}{I} \rceil, m-I\lfloor \frac{m}{I} \rfloor}$ denote the power vector for user-m; let $\hat{\mathbf{w}}_m = \hat{\mathbf{w}}_{\lceil \frac{m}{I} \rceil, m-I\lfloor \frac{m}{I} \rfloor}$ is the normalized beamforming vector for user-m; let $\overrightarrow{\gamma}_m = \overrightarrow{\gamma}_{\lceil \frac{m}{I} \rceil, m-I\lfloor \frac{m}{I} \rfloor}$ indicate the SINR for user-m; let $\sigma_m^2 = \sigma^2_{\lceil \frac{m}{I} \rceil, m-I\lfloor \frac{m}{I} \rfloor}$ represent the noise variance for user-m, where $m = 1, \cdots, \bar{I}$, $n = 1, \cdots, \bar{I}$.

Then, the downlink SINR at the mth UT becomes

$$\overrightarrow{\gamma}_m = \frac{p_m \left\| \bar{\mathbf{h}}_{m,m}^H \hat{\mathbf{w}}_m \right\|^2}{\sum\limits_{n \neq m} p_n \left\| \bar{\mathbf{h}}_{n,m}^H \hat{\mathbf{w}}_n \right\|^2 + 1} \tag{4}$$

where $\bar{\mathbf{h}}_{n,m} = \frac{\mathbf{h}_{n,m}}{\sigma_m}$.

To ensure the performance of the cell edge users, the max–min SINR optimization problem, regrding the per-BS power, can be expressed as:

$$\begin{cases} \max\limits_{\{\hat{\mathbf{w}}_m, p_m\}} \min\limits_m \overrightarrow{\gamma}_m \\ s.t. \sum\limits_{m=(j-1)I+1}^{jI} p_m \leq P_j, p_m \geq 0, ||\hat{\mathbf{w}}_m|| = 1 \end{cases} \tag{5}$$

where P_j is the maximum allowable transmission power of the j-th BS.

3. Coordinated Beamforming for Multi-Cell

The problem (5) is non-convex, and it is difficult to obtain an globally optimal solution.

By introducing some auxiliary variables $\{v_j\}_{j=1}^K$, we can transform the optimization problem (5) into the following problem (6):

$$\begin{cases} \min\limits_{v_j} \max\limits_{\{\hat{\mathbf{w}}_m, p_m\}} \min\limits_m \overrightarrow{\gamma}_m \\ s.t. \sum\limits_{m=1}^{\bar{I}} v_{\lceil \frac{m}{I} \rceil} p_m \leq \sum\limits_{j=1}^{K} v_j P_j, p_m \geq 0, ||\hat{\mathbf{w}}_m|| = 1 \end{cases} \tag{6}$$

By exploiting the extending uplink–downlink duality in [23,24,26], the downlink optimization problem (6) is transformed into the uplink optimization problem, as follows:

$$\begin{cases} \min\limits_{v_j} \max\limits_{\{\hat{\mathbf{w}}_m, \lambda_m\}} \min\limits_m \overleftarrow{\gamma}_m \\ s.t. \sum\limits_{m=1}^{\bar{I}} \lambda_m \leq \sum\limits_{j=1}^{K} v_j P_j, \lambda_m \geq 0, ||\hat{\mathbf{w}}_m|| = 1 \end{cases} \tag{7}$$

where λ_m refers to the convey power of the virtual uplink user-m, and $\overleftarrow{\gamma}_m$ indicates the uplink SINR of the m-th user, which can be expressed as

$$\overleftarrow{\gamma}_m = \frac{\lambda_m \left\| \bar{\mathbf{h}}_{m,m}^H \hat{\mathbf{w}}_m \right\|^2}{\sum\limits_{n=1, n \neq m}^{\bar{I}} \lambda_n \left\| \bar{\mathbf{h}}_{m,n}^H \hat{\mathbf{w}}_m \right\|^2 + v_{\lceil \frac{m}{I} \rceil}} \tag{8}$$

Owing to the convexity in v_j of the optimization problem (6), variable v_j can be obtained by exploiting the subgradient projection approach, and the subgradient of v_j is given by $\mathbf{g} = \left[P_1 - \sum\limits_{k=1}^{I} p_{1,k}, \cdots, P_K - \sum\limits_{k=1}^{I} p_{K,k} \right]$.

Based on the decoupling of the problem (7) with the fixed power, the optimal receiver beamforming that maximizes the SINR is the minimum mean-square error (MMSE) beamformer, which is usually computed as

$$\hat{\mathbf{w}}_m^{opt} = \frac{\left(\sum\limits_{n\neq m} \lambda_n \tilde{\mathbf{h}}_{m,n}\tilde{\mathbf{h}}_{m,n}^H + v_{\lceil \frac{m}{T} \rceil}\mathbf{I}_{M_{\lceil \frac{m}{T} \rceil}}\right)^{-1}\tilde{\mathbf{h}}_{m,m}}{\left\|\left(\sum\limits_{n\neq m} \lambda_n \tilde{\mathbf{h}}_{m,n}\tilde{\mathbf{h}}_{m,n}^H + v_{\lceil \frac{m}{T} \rceil}\mathbf{I}_{M_{\lceil \frac{m}{T} \rceil}}\right)^{-1}\tilde{\mathbf{h}}_{m,m}\right\|} \tag{9}$$

where $\tilde{\mathbf{h}}_{m,n} = \frac{\hat{\mathbf{h}}_{m,n}}{\sigma_m}$.

The existing result in [26] has revealed that we can iteratively update the uplink power as:

$$\lambda_m = \overleftarrow{\gamma}_m \frac{\left(\sum\limits_{n=1,n\neq m}^{\bar{I}} \lambda_n \left\|\bar{\mathbf{h}}_{m,n}^H \hat{\mathbf{w}}_m\right\|^2 + v_{\lceil \frac{m}{T} \rceil}\right)}{\left\|\bar{\mathbf{h}}_{m,m}^H \hat{\mathbf{w}}_m\right\|^2} \tag{10}$$

Utilizing the uplink–downlink duality theory in [23,24,26], we have

$$\begin{cases} \overrightarrow{\gamma}_m = \overleftarrow{\gamma}_m, \forall m \\ \sum\limits_{m=1}^{\bar{I}} v_{\lceil \frac{m}{T} \rceil} p_m = \sum\limits_{m=1}^{\bar{I}} \lambda_m \end{cases} \tag{11}$$

Some mathematical calculations can yield the following:

$$\mathbf{p} = \mathbf{DGp} + \mathbf{D1}_{\bar{I}} \tag{12}$$

$$\sum_{m=1}^{\bar{I}} v_{\lceil \frac{m}{T} \rceil} p_m = \sum_{m=1}^{\bar{I}} \lambda_m \tag{13}$$

where

$$\mathbf{G}_{m,n} = \begin{cases} 0 & m = n \\ \left\|\bar{\mathbf{h}}_{n,m}^H \hat{\mathbf{w}}_n\right\|^2 & m \neq n \end{cases} \tag{14}$$

$$\mathbf{D}_{m,n} = \begin{cases} \frac{\overleftarrow{\gamma}_m}{\left\|\bar{\mathbf{h}}_{m,m}^H \hat{\mathbf{w}}_m\right\|^2} & m = n \\ 0 & m \neq n \end{cases} \tag{15}$$

By multiplying either side of (12) by $\tilde{\mathbf{v}}^T$ and using (13), we have

$$1 = \frac{1}{\sum\limits_{m=1}^{\bar{I}} \lambda_m}\tilde{\mathbf{v}}^T\mathbf{DGp} + \frac{1}{\sum\limits_{m=1}^{\bar{I}} \lambda_m}\tilde{\mathbf{v}}^T\mathbf{D1}_{\bar{I}} \tag{16}$$

where $\tilde{\mathbf{v}} = (\underbrace{v_1 \cdots v_1}_{I}\underbrace{v_2 \cdots v_2}_{I}\cdots\underbrace{v_K \cdots v_K}_{I})^T$.

Defining an extended power vector $\tilde{\mathbf{p}} = \begin{bmatrix} \mathbf{p} \\ 1 \end{bmatrix}$, that is, $\tilde{\mathbf{p}}_{\bar{I}+1} = 1$, and the additional matrix:

$$\mathbf{Q} = \begin{bmatrix} \mathbf{DG} & \mathbf{D1}_{\bar{I}} \\ \frac{1}{\sum\limits_{m=1}^{\bar{I}} \lambda_m}\tilde{\mathbf{v}}^T\mathbf{DG} & \frac{1}{\sum\limits_{m=1}^{\bar{I}} \lambda_m}\tilde{\mathbf{v}}^T\mathbf{D1}_{\bar{I}} \end{bmatrix} \tag{17}$$

By combining (12) and (16), we have $\tilde{\mathbf{p}} = \mathbf{Q}\tilde{\mathbf{p}}$. By exploiting the conclusions in [24], it is clear that we have the optimal power vector $\mathbf{p}$, which indicates the maximum components of the dominant eigenvector of $\mathbf{Q}$. The developed scheme is summarized as follows.

4. Analysis of the Large System

From the above Algorithm 1, we know that, although the beamforming vectors can be efficiently calculated based on its closed-form structure, the uplink–downlink power needs to by instantaneously iteratively updated with the instantaneous CSI. For the massive MIMO system, the amount of instantaneous power updates can be impractically large. In response, we aim to acheive a max–min SINR optimization algorithm design that only requires statistical CSI to update the uplink–downlink power and that can obtain the MMSE beamformer without iteration.

Algorithm 1 Coordinated Beamforming for Multi-cell

(1) Initialize $\mathbf{v}[0] \in R_{+}^{\bar{I}}$, $i = 0$;

(2) Initialize $\boldsymbol{\lambda}[0] \in R_{+}^{\bar{I}}$, $\hat{\mathbf{w}}_m[0] \in \mathbb{C}^{M\lceil \frac{m}{\bar{I}} \rceil \times \bar{I}} \forall m$ such that $\sum_{\mathrm{m}=1}^{\bar{I}} \lambda_m[0] \leq \sum_{j=1}^{K} v_j[i]P_j$, $||\hat{\mathbf{w}}_m[0]|| = 1$, $l = 0$;

(3) Let $l = l + 1$; update uplink power $\boldsymbol{\lambda}[l]$:

$$\lambda_m[l] = \frac{1}{\overleftarrow{\Upsilon}_m(\mathbf{v}[i], \boldsymbol{\lambda}[l-1], \hat{\mathbf{w}}_m[l-1])}\lambda_m[l-1] \qquad \forall m$$

(4) Normalize $\boldsymbol{\lambda}[l]$:

$$\boldsymbol{\lambda}[l] \leftarrow \frac{\sum_{j=1}^{K} v_j[i]P_j}{\sum_{\mathrm{m}=1}^{\bar{I}} \lambda_m[l]}\boldsymbol{\lambda}[l]$$

(5) According to (9), update the transmit beamformer $\hat{\mathbf{w}}_m[l]$;

(6) If $|\boldsymbol{\lambda}[l] - \boldsymbol{\lambda}[l-1]| > \varepsilon$, return to step (3); otherwise, go to step (7);

(7) According to (14), (15), (17), compute $\mathbf{G}_{m,n}$, $\mathbf{D}_{m,n}$ and $\mathbf{Q}$;

(8) Update downlink power $\mathbf{p}$:

$$\mathbf{p} = \left[\mathbf{f}_{\max}/(\mathbf{f}_{\max})_{\bar{I}+1}\right]_{1\sim\bar{I}}$$

(9) Let $i = i + 1$, Optimize $\mathbf{v}[i]$: $\mathbf{v}[i] = \mathbf{v}[i-1] - \varsigma\mathbf{g}$ with the subgradient method. If $|\mathbf{v}[i] - \mathbf{v}[i-1]| > \delta$, return to step (2); otherwise, the iteration stops.

Combining (9) and (8), we have

$$\overleftarrow{\gamma}_m = \lambda_m \bar{\mathbf{h}}_{m,m}^H \left(\sum_{n \neq m} \lambda_n \tilde{\mathbf{h}}_{m,n} \tilde{\mathbf{h}}_{m,n}^H + v_{\lceil \frac{m}{\bar{I}} \rceil} \mathbf{I}_{M\lceil \frac{m}{\bar{I}} \rceil} \right)^{-1} \bar{\mathbf{h}}_{m,m} \forall m \tag{18}$$

Moreover, the asymptotic approximation for $\overleftarrow{\gamma}_m$ only includes statistical CSI, which mainly focuses on the empirical distribution of the eigenvalue for $\left(\sum_{n \neq m} \lambda_n \tilde{\mathbf{h}}_{m,n} \tilde{\mathbf{h}}_{m,n}^H + v_{\lceil \frac{m}{\bar{I}} \rceil} \mathbf{I}_{M\lceil \frac{m}{\bar{I}} \rceil} \right)^{-1}$.

Lemma 1. *When the system dimension* $M_{\lceil \frac{m}{I} \rceil} \to \infty$, *there exists* $\overleftarrow{\mathrm{Y}}_m - \overleftarrow{\gamma}_m \overrightarrow{M_{\lceil \frac{m}{I} \rceil} \to \infty} 0$, *where*

$$\overleftarrow{\mathrm{Y}}_m = \lambda_m tr\left(\bar{\mathbf{\Phi}}_{m,m}\left(\sum_{n\neq m}\lambda_n \tilde{\mathbf{h}}_{m,n}\tilde{\mathbf{h}}_{m,n}^H + v_{\lceil \frac{m}{I} \rceil}\mathbf{I}_{M_{\lceil \frac{m}{I} \rceil}}\right)^{-1}\right)$$

$\overleftarrow{\mathrm{Y}}_m$ *is also modeled by the following equation:*

$$\overleftarrow{\mathrm{Y}}_m = \lambda_m \frac{1}{\bar{I}} tr(\bar{\mathbf{\Phi}}_{m,m}\mathbf{T}_m) \quad \forall m \tag{19}$$

where

$$\bar{\mathbf{\Phi}}_{m,m} = \frac{\mathbf{\Phi}_{m,m}}{\sigma_m^2} = \frac{d_{m,m}}{\sigma_m^2 M_{\lceil \frac{m}{I} \rceil}}\mathbf{R}_{m,m}$$

$$\mathbf{T}_m = \left(\frac{1}{\bar{I}}\sum_{n=1,n\neq m}^{\bar{I}}\lambda_n \bar{\mathbf{\Phi}}_{m,n}\frac{1}{1+\delta_n} + \frac{1}{\bar{I}}v_{\lceil \frac{m}{I} \rceil}\mathbf{I}_{M_{\lceil \frac{m}{I} \rceil}}\right)^{-1}$$

$$\delta_n = \frac{1}{\bar{I}} tr(\lambda_n \bar{\mathbf{\Phi}}_{m,n}\boldsymbol{T}_m)$$

Proof. This can easily be proven by Lemmas A1 and A2 in Appendix A.1. □

According to the results of [23,24,26], once the optimal solution to the problem is obtained, each user has the same SINR. Thus, we have

$$\lambda_m = \frac{\overleftarrow{\mathrm{Y}}_m}{\frac{1}{\bar{I}} tr(\bar{\mathbf{\Phi}}_{m,m}\mathbf{T}_m)} \quad \forall m \tag{20}$$

Theorem 1. *The instantaneous extended coupling matrix* $\mathbf{G}$ *and* $\mathbf{D}$ *can be approximated by a deterministic matrix* $\tilde{\mathbf{G}}$ *and* $\tilde{\mathbf{D}}$ *such that* $\tilde{\mathbf{G}}_{m,n} - \mathbf{G}_{m,n}\overrightarrow{M_{\lceil \frac{m}{I} \rceil} \to \infty} 0$ *and* $\tilde{\mathbf{D}}_{m,n} - \mathbf{D}_{m,n}\overrightarrow{M_{\lceil \frac{m}{I} \rceil} \to \infty} 0$, *respectively, as the system dimension* $M_{\lceil \frac{m}{I} \rceil} \to \infty$. $\tilde{\mathbf{G}}$ *and* $\tilde{\mathbf{D}}$ *are expressed as*

$$\tilde{\mathbf{G}}_{m,n} = \begin{cases} 0 & m = n \\ \frac{\frac{1}{I} tr(\bar{\mathbf{\Phi}}_{n,n}\mathbf{T}_n\bar{\mathbf{\Phi}}_{n,m}\mathbf{T}_n)}{tr\left(\bar{\mathbf{\Phi}}_{n,n}\mathbf{T}_n'\right)\left(1+\lambda_m \frac{1}{I} tr(\bar{\mathbf{\Phi}}_{n,m}\mathbf{T}_n)\right)^2} & m \neq n \end{cases} \tag{21}$$

$$\tilde{\mathbf{D}}_{m,n} = \begin{cases} \frac{\overleftarrow{\mathrm{Y}}_m tr\left(\bar{\mathbf{\Phi}}_{m,m}\mathbf{T}_m'\right)}{\frac{1}{I}\left(\sqrt{1-\tau^2}tr(\bar{\mathbf{\Phi}}_{m,m}\mathbf{T}_m)\right)^2} & m = n \\ 0 & m \neq n \end{cases} \tag{22}$$

where

$$\mathbf{T}_m' = \mathbf{T}_m\left(\frac{1}{\bar{I}}\sum_{n=1,n\neq m}^{\bar{I}}\lambda_n \bar{\mathbf{\Phi}}_{m,n}\frac{\delta_n'}{(1+\delta_n)^2} + \mathbf{I}_{M_{\lceil \frac{m}{I} \rceil}}\right)\mathbf{T}_m$$

$$\delta_n' = \frac{1}{\bar{I}} tr\left(\lambda_n \bar{\mathbf{\Phi}}_{m,n}\mathbf{T}_m'\right)$$

Proof. The proof is presented in Appendix A.2. □

Then, the extended coupling matrix $\tilde{\mathbf{Q}}$, which only is related to the statistical CSI, can be obtained as follows

$$\tilde{\mathbf{Q}} = \begin{bmatrix} \tilde{\mathbf{D}}\tilde{\mathbf{G}} & \tilde{\mathbf{D}}\mathbf{1}_{\bar{I}} \\ \frac{1}{\sum_{m=1}^{\bar{I}} \lambda_m} \tilde{\mathbf{v}}^T \tilde{\mathbf{D}}\tilde{\mathbf{G}} & \frac{1}{\sum_{m=1}^{\bar{I}} \lambda_m} \tilde{\mathbf{v}}^T \tilde{\mathbf{D}}\mathbf{1}_{\bar{I}} \end{bmatrix} \tag{23}$$

Therefore, the downlink transmit power can be obtained by the extended coupling matrix $\tilde{\mathbf{Q}}$, similar to Section 3.

The subgradient method to update the virtual noise variance $\mathbf{v}$ is convergent by the convexity of the optimization problem (6); that is, the outer iteration is convergent. According to the deterministic equivalents [26], we know that $\boldsymbol{\lambda}$ and $\mathbf{p}$ can converge to a constant point in the large system, indicating that the inner iteration is convergent.

5. Simulation Results

In this section, we investigate the performance of our developed schemes via numerical simulations. We considered a three-cell cluster where the distance between BSs was 1 km. All users of the considered system were randomly located at the cell edge. The distance from the related BS was set as 400 m. The path loss (in dB) model was supposed to be $15.3 + 37.6\log_{10} d$ for distance d in meters.

However, the general, the antenna of each BS and the number of receivers were set as M and I, respectively. Moreover, the covariance matrix was expressed as

$$[\mathbf{R}_{m,l,k}]_{i,j} = \begin{cases} r^{j-i}, & i < j \\ \left(r^{i-j}\right)^*, & i \geq j \end{cases} \tag{24}$$

where $i = 1, 2, \cdots, M$, $j = 1, 2, \cdots, M$, $r = 0.1$.

Figures 2 and 3 show a comparison of the downlink SINR achieved using the optimal beamformer in the Algorithm 1, the asymptotically optimal beamformer in the Algorithm 2, and the optimal beamformer for perfect CSI and the MRT with respect to the different values of the per-BS power constraint P. As can be seen from Figure 2, the asymptotic optimal SINR is very close to the optimal SINR value, both are very close to the SINR value in the case of perfect channel information, and both are better than the worst and average SINR of MRT. It can be seen from Figure 3 that, due to the increase in channel correlation, although the difference between the progressive optimal SINR, the optimal SINR and the SINR under perfect channel information is slightly larger than that in Figure 2, they are still very close and better than the worst and average SINR of MRT.

Figures 4 and 5 show a comparison of the downlink SINR achieved using the optimal beamformer in the Algorithm 1, the asymptotically optimal beamformer in the Algorithm 2, and the optimal beamformer for perfect CSI and the MRT with respect to different values of the per-BS power constraint P. The worst SINR of MRT was achieved under the constraints of equal power allocation. The average SINR of MRT was achieved under the constraints of max–min SINR power allocation. In Figures 4 and 5, the application of an asymptotic beamformer could be almost the same as the application of an optimal beamformer, and both of these are better than MRT. Moreover, both were close to the optimal beamformer for perfect CSI. Therefore, the Algorithms 1 and 2 are robust to channel estimation errors. At the same time, compared with Figures 4 and 5, although the SINR difference was slightly increased, the performance was still good, which fully illustrates the effectiveness of the algorithm. Figure 6 plots the SINR with regard to I, which indicates that the SINR first increases and then decreases with I. To relieve this problem, more transmitters need to be equipped with transmit antennas.

Algorithm 2 Power Allocation for Multi-Cell MU-MISO System

(1) Initialize $\mathbf{v}[0] \in R_{+}^{\bar{I}}$, $i = 0$;

(2) Initialize $\boldsymbol{\lambda}[0] \in R_{+}^{\bar{I}}$ such that $\sum_{\mathrm{m}=1}^{\bar{I}} \lambda_m[0] \leq \sum_{j=1}^{K} v_j[i]P_j$, $l = 0$;

(3) Let $l = l + 1$, update uplink power $\boldsymbol{\lambda}[l]$:

$$\lambda_m[l] = \frac{1}{\overleftarrow{\mathrm{Y}}_m(\mathbf{v}[i], \boldsymbol{\lambda}[l-1])}\lambda_m[l-1] \ \forall m$$

(4) Normalize $\boldsymbol{\lambda}[l]$:

$$\boldsymbol{\lambda}[l] \leftarrow \frac{\sum_{j=1}^{K} v_j[i]P_j}{\sum_{\mathrm{m}=1}^{\bar{I}} \lambda_m[l]}\boldsymbol{\lambda}[l]$$

(5) If $|\boldsymbol{\lambda}[l] - \boldsymbol{\lambda}[l-1]| > \varepsilon$, return to step (3); otherwise, go to step (6);

(6) Update $\mathbf{T}_{\mathrm{m}}[l]$ and $\mathbf{T}_{m}^{'}[l]$;

(7) According to (21)–(23), compute $\tilde{\mathbf{G}}_{m,n}$, $\tilde{\mathbf{D}}_{m,n}$ and $\tilde{\mathbf{Q}}$;

(8) Update downlink power $\mathbf{p}$:

$$\mathbf{p} = \left[\mathbf{f}_{\max}/(\mathbf{f}_{\max})_{\bar{I}+1}\right]_{1\sim\bar{I}}$$

(9) Let $i = i + 1$, optimize $\mathbf{v}[i]$: $\mathbf{v}[i] = \mathbf{v}[i-1] - \varsigma\mathbf{g}$ with the subgradient method. If $|\mathbf{v}[i] - \mathbf{v}[i-1]| > \delta$, return to step (2); otherwise, the iteration stops.

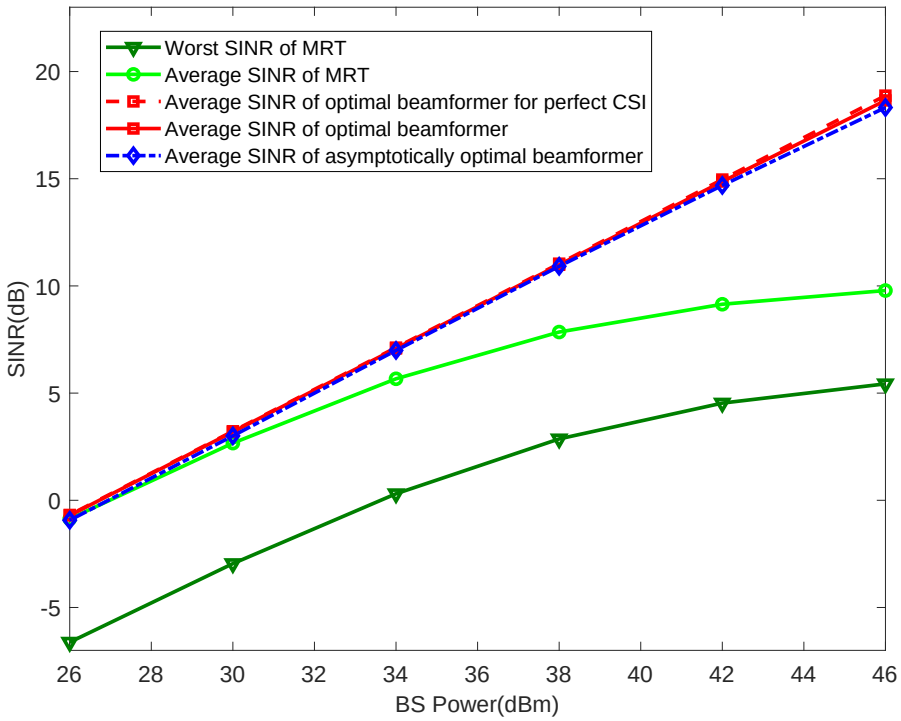

Figure 2. The achieved SINR among several algorithms with regard to P ($M = 64$, $I = 4$, $K = 3$, $r = 0.1$, $\tau = 0.07$).

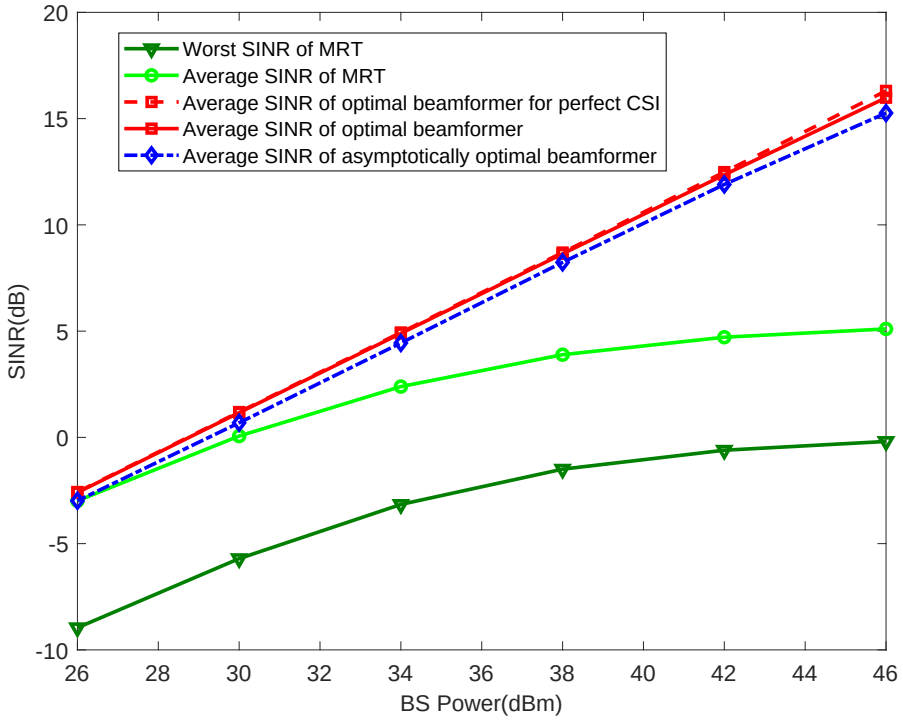

Figure 3. The achieved SINR among several algorithms with regard to P ($M = 64$, $I = 4$, $K = 3$, $r = 0.7$, $\tau = 0.07$).

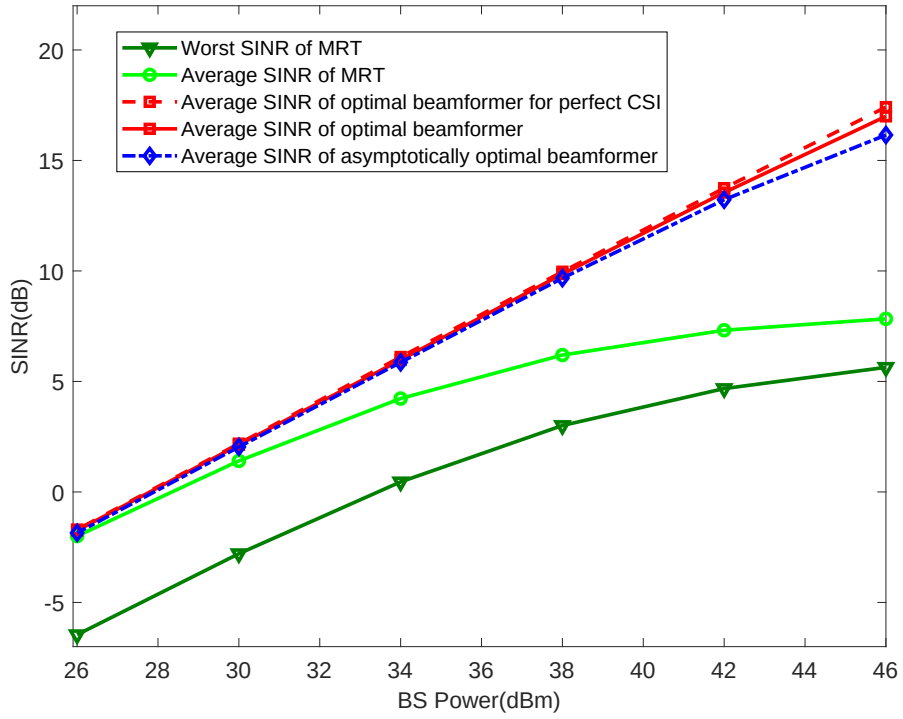

Figure 4. The achieved SINR among several algorithms with regard to P ($M = 64$, $I = 4$, $K = 3$, $r = 0.1$, $\tau = 0.1$).

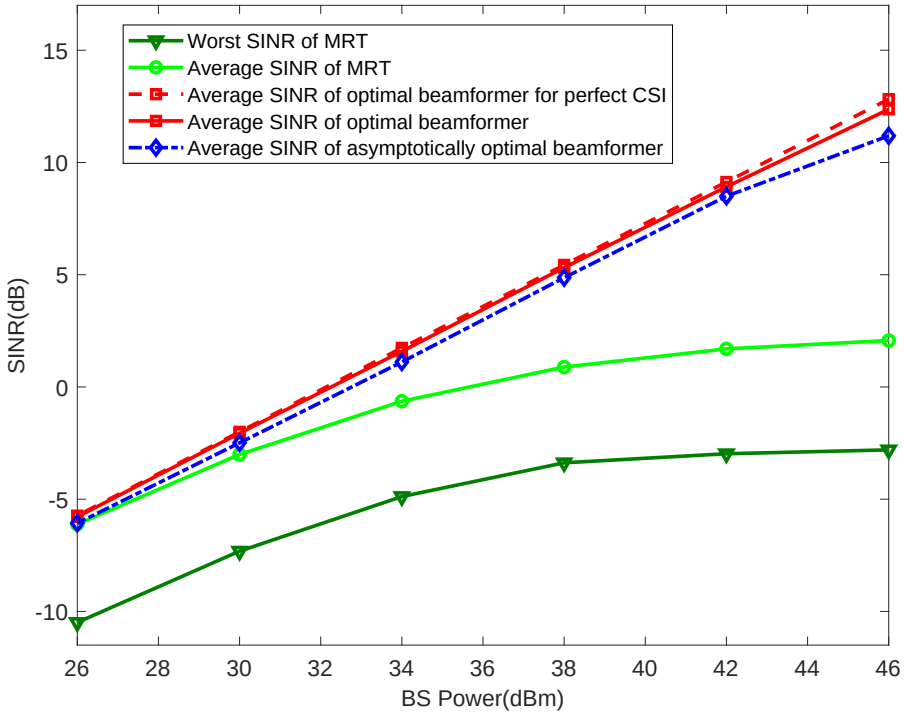

Figure 5. The achieved SINR among several algorithms with regard to P ($M = 64$, $I = 4$, $K = 3$, $r = 0.7$, $\tau = 0.1$).

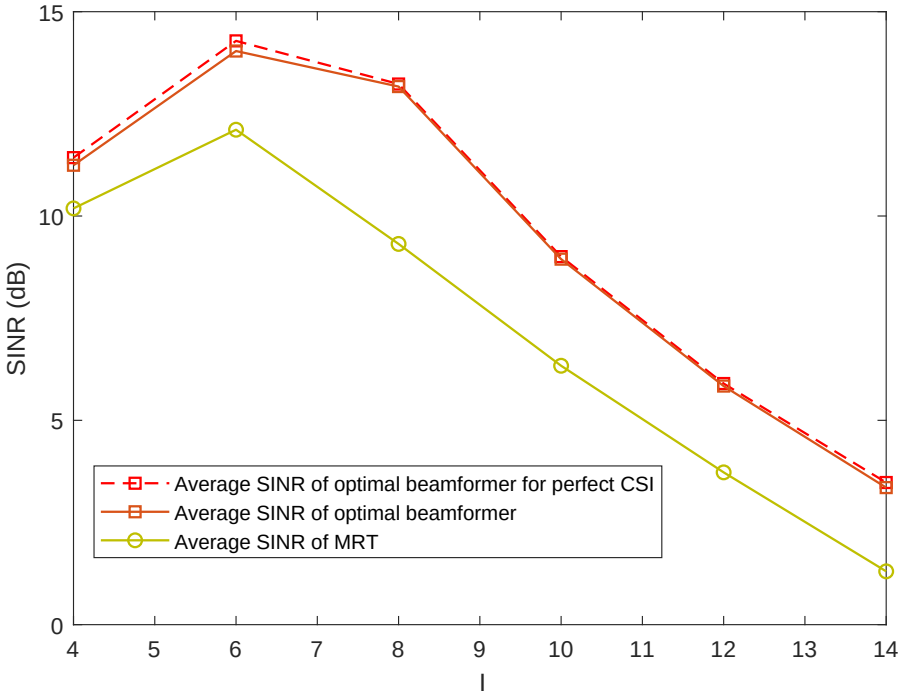

Figure 6. The achieved SINR among several algorithms with regard to I ($M = 64$, $P = 30$, $K = 3$, $r = 0.7$, $\tau = 0.1$).

Figure 7 considers that the per-BS power constraint is $P = 46$ dBm and demonstrates a comparison of the downlink SINR achieved using the optimal beamformer, the asymptotically optimal beamformer, the optimal beamformer for perfect CSI and the MRT with respect to different BS antenna numbers M. The worst SINR of MRT and the average SINR of MRT were both achieved under the constraints of equal power allocation. In Figure 7,

not only was the performance of the asymptotic beamformer close to the performance of the optimal beamformer and better than MRT, the performance of the asymptotic optimal beamformer improved with the growth in BS antennas. Furthermore, the performance of the asymptotic optimal beamformer was the same as the performance of the optimal beamformer for perfect CSI.

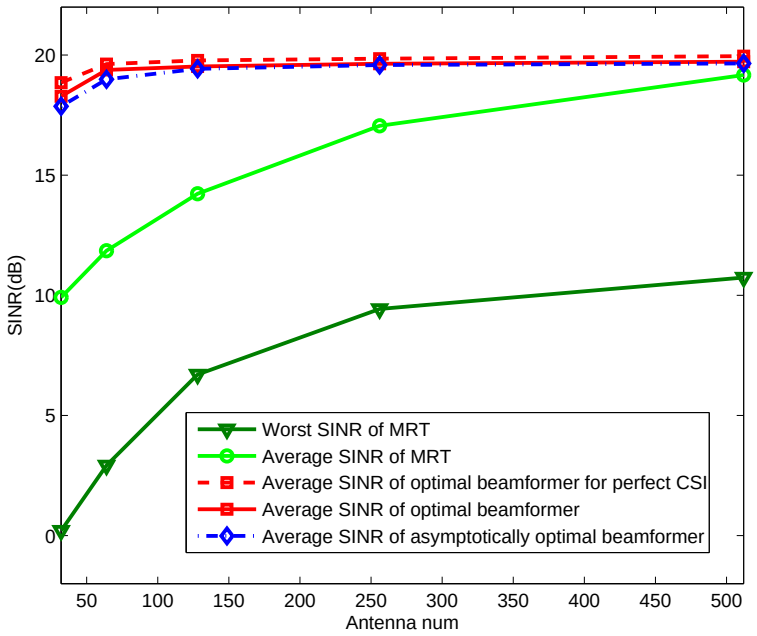

Figure 7. The achieved SINR among several algorithms with regard to M (I = 4, K = 3, τ = 0.1, P = 46 dBm).

6. Conclusions

In this paper, we investigated the coordinated beamformer design for large-scale MIMO dense systems with imperfect CSI. The original optimization problem belongs to a non-convex optimization problem, so it is difficult to directly solve. By introducing several slack parameters, the original downlink optimization problem with the coupling variables can be transformed into an equivalent dual uplink optimization problem. Then, we proposed an instantaneous updating uplink–downlink power algorithm, which relies on instantaneous channel state information for the finite system. Instead, the downlink power can be directly calculated by the extended coupling matrix, without iterations. For the massive MIMO network, to handle the problem of power needing to instantaneously update, we proposed the updating uplink–downlink power algorithm. This only requires statistical CSI by applying the random matrix theory, and the beamforming can be calculated directly based on the obtained uplink power and available local instantaneous CSI. Finally, each user's SINR can be achieved. The simulation results show the effectiveness of the induced algorithms.

Author Contributions: B.Y. proposed the CSI-Impair algorithm, designed the simulation scheme and wrote the paper. Z.R. gave suggestions on the proposed algorithm and helped to improve the quality of the final manuscript. S.T. helped to perform the simulation tests and analyzed the results. All authors have read and agreed to the published version of the manuscript.

Funding: The works was supported by the The National Key R&D Program of China (2017YFF0205500).

Institutional Review Board Statement: Not applicable.

Informed Consent Statement: Not applicable.

Data Availability Statement: Data will be provided upon request.

Conflicts of Interest: The authors declare no conflict of interest.

Appendix A

Appendix A.1. Related Lemmas

Lemma A1 ([27]). *Let* $\mathbf{x} \sim \mathcal{CN}(\mathbf{0}, \mathbf{I}_M)$ *and* $\mathbf{U} \in \mathbb{C}^{M \times M}$ *is Hermitian, then* $\frac{1}{M}\mathbf{x}^H\mathbf{U}\mathbf{x} - \frac{1}{M}tr(\mathbf{U}) \xrightarrow{M_{\lceil \frac{m}{I} \rceil} \to \infty} 0$.

Lemma A2 ([25]). *If* $\mathbf{U} \in \mathbb{C}^{M \times M}$ *is Hermitian matrix and* $\mathbf{H} \in \mathbb{C}^{M \times \bar{I}}$ *is the random matrix that meets* $\mathbf{H}_n \sim \mathcal{CN}(0, \mathbf{\Phi}_{m,n})$. *Then, the following formulation for any* $z > 0$ *holds:*

$$\frac{1}{\bar{I}}tr(\mathbf{U}\mathbf{\Sigma}(\boldsymbol{z})) - \frac{1}{\bar{I}}tr(\mathbf{U}\mathbf{T}(z)) \xrightarrow{M_{\lceil \frac{m}{I} \rceil} \to \infty} 0$$

where

$$\mathbf{\Sigma}(z) = \left(\mathbf{H}\mathbf{H}^H - z\mathbf{I}_M\right)^{-1}$$

$$\mathbf{T}(z) = \left(\frac{1}{\bar{I}}\sum_{n=1}^{\bar{I}} \frac{\mathbf{\Phi}_{m,n}}{1+\delta_n(z)} - z\mathbf{I}_M\right)^{-1}$$

$$\delta_n(z) = \frac{1}{\bar{I}}tr(\mathbf{\Phi}_{m,n}\mathbf{T}(z))$$

Appendix A.2. Proof of Theorem 1

To remove the influence of the small-scale fading parameters of matrix $\mathbf{G}$ and $\mathbf{D}$, we need to obtain the deterministic approximation of $\left\|\bar{\mathbf{h}}_{m,m}^H\hat{\mathbf{w}}_m\right\|^2$ and $\left\|\bar{\mathbf{h}}_{n,m}^H\hat{\mathbf{w}}_n\right\|^2$ for the massive MIMO system. According to the beamforming in (9) and the Lemma A1, we have:

$$\left\|\bar{\mathbf{h}}_{m,m}^H\hat{\mathbf{w}}_m\right\|^2 \xrightarrow{M_{\lceil \frac{m}{I} \rceil} \to \infty} \frac{1}{\bar{I}}\frac{\left(\sqrt{1-\tau^2}tr(\bar{\mathbf{\Phi}}_{m,m}\mathbf{T}_m)\right)^2}{tr\left(\bar{\mathbf{\Phi}}_{m,m}\mathbf{T}_m'\right)}$$

where

$$\bar{\mathbf{\Phi}}_{m,m} = \frac{\mathbf{\Phi}_{m,m}}{\sigma_m^2} = \frac{d_{m,m}}{\sigma_m^2 M_{\lceil \frac{m}{I} \rceil}}\mathbf{R}_{m,m}$$

$$\mathbf{T}_m = \left(\frac{1}{\bar{I}}\sum_{n=1,n\neq m}^{\bar{I}} \lambda_n\bar{\mathbf{\Phi}}_{m,n}\frac{1}{1+\delta_n} + \frac{1}{\bar{I}}v_{\lceil \frac{m}{I} \rceil}\mathbf{I}_{M_{\lceil \frac{m}{I} \rceil}}\right)^{-1}$$

$$\delta_n = \frac{1}{\bar{I}}tr(\lambda_n\bar{\mathbf{\Phi}}_{m,n}\mathbf{T}_m)$$

$$\mathbf{T}_m' = \mathbf{T}_m\left(\frac{1}{\bar{I}}\sum_{n=1,n\neq m}^{\bar{I}} \lambda_n\bar{\mathbf{\Phi}}_{m,n}\frac{\delta_n'}{(1+\delta_n)^2} + \mathbf{I}_{M_{\lceil \frac{m}{I} \rceil}}\right)\mathbf{T}_m$$

$$\delta_n' = \frac{1}{\bar{I}}tr\left(\lambda_n\bar{\mathbf{\Phi}}_{m,n}\mathbf{T}_m'\right)$$

By exploiting the Rank-1 Perturbation Lemma [28] and the Lemma A2, we can obtain:

$$\left\|\overline{\mathbf{h}}_{n,m}^{H}\mathbf{w}_n\right\|^2 = \frac{\overline{\mathbf{h}}_{n,m}^{H}\Xi_n^{-1}\overline{\mathbf{h}}_{n,n}\overline{\mathbf{h}}_{n,n}^{H}\Xi_n^{-1}\overline{\mathbf{h}}_{n,m}}{\overline{\mathbf{h}}_{n,n}^{H}\Xi_n^{-2}\overline{\mathbf{h}}_{n,n}}$$
$$= \frac{\overline{\mathbf{h}}_{n,m}^{H}\Theta_n^{-1}\overline{\mathbf{h}}_{n,n}\overline{\mathbf{h}}_{n,n}^{H}\Theta_n^{-1}\overline{\mathbf{h}}_{n,m}}{\overline{\mathbf{h}}_{n,n}^{H}\Xi_n^{-2}\overline{\mathbf{h}}_{n,n}\left(1+\lambda_m\overline{\mathbf{h}}_{n,m}^{H}\Theta_n^{-1}\overline{\mathbf{h}}_{n,m}\right)^2}$$
$$\xrightarrow[M_{\lceil\frac{m}{I}\rceil}\to\infty]{} \frac{\frac{1}{I}tr(\bar{\mathbf{\Phi}}_{n,n}\mathbf{T}_n\bar{\mathbf{\Phi}}_{n,m}\mathbf{T}_n)}{tr\left(\bar{\mathbf{\Phi}}_{n,n}\mathbf{T}_n'\right)\left(1+\lambda_m\frac{1}{I}tr(\bar{\mathbf{\Phi}}_{n,m}\mathbf{T}_n)\right)^2}$$

where $\mathbf{\Theta}_n = \left(\sum_{j\neq n,m}\lambda_j\tilde{\mathbf{h}}_{n,j}\tilde{\mathbf{h}}_{n,j}^{H} + v_{\lceil\frac{n}{I}\rceil}\mathbf{I}_{M_{\lceil\frac{n}{I}\rceil}}\right)^{-1}$.

Thus, the elements of the $\tilde{\mathbf{G}}$ and $\tilde{\mathbf{D}}$ matrixes with the channel estimation error can be calculated as follows:

$$\tilde{\mathbf{G}}_{m,n} = \begin{cases} 0 & m = n \\ \frac{\frac{1}{I}tr(\bar{\mathbf{\Phi}}_{n,n}\mathbf{T}_n\bar{\mathbf{\Phi}}_{n,m}\mathbf{T}_n)}{tr\left(\bar{\mathbf{\Phi}}_{n,n}\mathbf{T}_n'\right)\left(1+\lambda_m\frac{1}{I}tr(\bar{\mathbf{\Phi}}_{n,m}\mathbf{T}_n)\right)^2} & m \neq n \end{cases}$$

$$\tilde{\mathbf{D}}_{m,n} = \begin{cases} \frac{\overleftarrow{\Upsilon}_m tr\left(\bar{\mathbf{\Phi}}_{m,m}\mathbf{T}_m'\right)}{\frac{1}{I}\left(\sqrt{1-\tau^2}tr(\bar{\mathbf{\Phi}}_{m,m}\mathbf{T}_m)\right)^2} & m = n \\ 0 & m \neq n \end{cases}$$

References

1. Zhao, B.; Cui, Q.; Liang, S.; Zhai, J.; Hou, Y.; Huang, X.; Pan, M.; Tao, X. Green concerns in federated learning over 6G. *China Commun.* **2022**, *19*, 50–69. [CrossRef]
2. Bi, Q. Ten Trends in the Cellular Industry and an Outlook on 6G. *IEEE Commun. Mag.* **2019**, *57*, 31–36. [CrossRef]
3. Yang, X.; Zhou, Z.; Huang, B. URLLC Key Technologies and Standardization for 6G Power Internet of Things. *IEEE Commun. Stand. Mag.* **2021**, *5*, 52–59. [CrossRef]
4. Elbayoumi, M.; Hamouda, W.; Youssef, A. Edge Computing and Multiple-Association in Ultra-Dense Networks: Performance Analysis. *IEEE Trans. Commun.* **2022**, *70*, 5098–5112. [CrossRef]
5. Jiang, H.; Wang, H.; Hu, Y.; Wu, J. Dynamic User Association in Scalable Ultra-Dense LEO Satellite Networks. *IEEE Trans. Veh. Technol.* **2022**, *71*, 8891–8905. [CrossRef]
6. Gao, Y.; Zhang, H.; Yu, F.; Xia, Y.; Shi, Y. Joint Computation Offloading and Resource Allocation for Mobile-Edge Computing Assisted Ultra-Dense Networks. *J. Commun. Inf. Netw.* **2022**, *7*, 96–106. [CrossRef]
7. Liu, W.; Liu, K.; Tian, L.; Zhang, C.; Yang, Y. Joint Interference Alignment and Subchannel Allocation in Ultra-Dense Networks. *IEEE Trans. Veh. Technol.* **2022**, *71*, 7287–7296. [CrossRef]
8. Kibinda, N.M.; Ge, X. User-Centric Cooperative Transmissions-Enabled Handover for Ultra-Dense Networks. *IEEE Trans. Veh. Technol.* **2022**, *71*, 4184–4197. [CrossRef]
9. Li, F.; Yao, H.; Du, H.; Jiang, C.; Han, Z.; Liu, Y. Auction Design for Edge Computation Offloading in SDN-Based Ultra Dense Networks. *IEEE Trans. Mob. Comput.* **2022**, *21*, 1580–1595. [CrossRef]
10. Gesbert, D.; Hanly, S.; Huang, H.; Shitz, S.; Simeone, O.; Yu, W. Multi-cell MIMO coopeative networks: A new look at interference. *IEEE J. Sel. Areas Commun.* **2010**, *28*, 1380–1408. [CrossRef]
11. Zhang, H.; Dai, H. Cochannel interferecence mitigation and cooperative processing in dwonlink multicell multiuser MIMO networks. *EURASIP J. Wirel. Commun. Netw.* **2004**, *2*, 222–235.
12. Wang, H.; Huang, Y.; He, S.; Yang, L. Power Minimization for Uplink RIS-Assisted CoMP-NOMA Networks with GSIC. *IEEE Trans. Veh. Technol.* **2020**, *69*, 3481–3485. [CrossRef]
13. Huang, W.; Liu, C.; Shi, Z.; Fu, Y.; Song, R. Cloud and Edge Multicast Beamforming for Cache-Enabled Ultra-Dense Networks. *IEEE Trans. Commun.* **2022**, *70*, 4559–4573. [CrossRef]
14. Rezvani, S.; Yamchi, N.; Javan, M.; Jorswieck, E. Resource Allocation in Virtualized CoMP-NOMA HetNets: Multi-Connectivity for Joint Transmission. *IEEE Trans. Commun.* **2021**, *69*, 4172–4185. [CrossRef]
15. Park, J.; Lee, N.; Heath, R.W. Cooperative Base Station Coloring for Pair-Wise Multi-Cell Coordination. *IEEE Trans. Commun.* **2016**, *64*, 402–415. [CrossRef]

16. Gelincik, J.; Wigger, M.; Wang, L. Benefits of Local Cooperation in Sectorized Cellular Networks Under a Complexity Constraint. *IEEE Trans. Wirel. Commun.* **2021**, *20*, 3897–3910. [CrossRef]
17. Dai, Y.; Liu, J.; Sheng, M.; Cheng, N.; Shen, X. Joint Optimization of BS Clustering and Power Control for NOMA-Enabled CoMP Transmission in Dense Cellular Networks. *IEEE Trans. Veh. Technol.* **2021**, *70*, 1924–1937. [CrossRef]
18. Zhao, J.; Yang, L.; Xia, M.; Motani, M. Unified Analysis of Coordinated Multipoint Transmissions in mmWave Cellular Networks. *IEEE Internet Things J.* **2022**, *9*, 12166–12180. [CrossRef]
19. Kasi, S.; Hamshmi, U.; Nabeel, M.; Ekin, S.; Imran, A. Analysis of Area Spectral and Energy Efficiency in a CoMP-Enabled User-Centric Cloud RAN. *IEEE Internet Things J.* **2021**, *5*, 1999–2015. [CrossRef]
20. Hu, S.; Xu, C.; Wang, X.; Huang, Y.; Zhang, S. A Stochastic ADMM Approach to Distributed Coordinated Multicell Beamforming for Renewables Powered Wireless Cellular Networks. *IEEE Trans. Veh. Technol.* **2018**, *67*, 8595–8607. [CrossRef]
21. Asgharimoghaddam, H.; Tolli, A.; Sanguinetti, L.; Debbah, M. Decentralizing Multicell Beamforming via Deterministic Equivalents. *IEEE Trans. Commun.* **2019**, *67*, 1894–1909. [CrossRef]
22. Xie, M.; Lok, T. SINR Balancing via Base Station Association, Beamforming, and Power Control in Downlink Multicell MISO Systems. *IEEE Trans. Wirel. Commun.* **2018**, *17*, 1811–1821. [CrossRef]
23. Nguyen, K.; Vu, Q.; Juntti, M.; Tran, L. Distributed Solutions for Energy Efficiency Fairness in Multicell MISO Downlink. *IEEE Trans. Wirel. Commun.* **2017**, *16*, 6232–6247. [CrossRef]
24. Schubert, M.; Boche, H. Solution of the multiuser downlink beamforming problem with individual SINR constraints. *IEEE Trans. Veh. Technol.* **2004**, *53*, 18–28. [CrossRef]
25. Wagner, S.; Couillet, R.; Debbah, M.; Slock, D.T.M. Large system analysis of linear precoding in correlated MISO broadcast channels under limited feedback. *IEEE Trans. Inf. Theory* **2012**, *58*, 4509–4537. [CrossRef]
26. Huang, Y.; Tan, C.W.; Rao, B.D. Joint beamforming and power control in coordinated multicell: max-min duality, effective network and large system transition. *IEEE Trans. Wirel. Commun.* **2013**, *12*, 2730–2742. [CrossRef]
27. Bai, Z.D.; Silverstein, J.W. No eigenvalue outside the support of the limiting spectral distribution of large dimensional sample covariance matrices. *Ann. Probab.* **1998**, *26*, 316–345. [CrossRef]
28. Silver, J.; Bai, Z. On the Empirical Distribution of Eigenvalues of a Class of Large Dimensional Random Matrices. *J. Multivar. Anal.* **1995**, *54*, 175–192.